# 1 How COVID-19 related policies reshaped organic aerosol

### source contributions in central London

3

2

4 Gang I. Chen<sup>1</sup>\*, Anja H. Tremper<sup>1</sup>, Max Priestman<sup>1</sup>, Anna Font<sup>2</sup>, and David C. Green<sup>1,3</sup>

5

MRC Centre for Environment and Health, Environmental Research Group, Imperial College
 London, 86 Wood Lane, London, W12 0BZ, UK

8

<sup>2</sup>IMT Nord Europe, Europe, Institut Mines-Télécom, Univ. Lille, Centre for Education, Research
 and Innovation in Energy Environment (CERI EE), 59000 Lille, France

11

- 12 <sup>3</sup>HPRU in Environmental Exposures and Health, Imperial College London, 86 Wood Lane,
- 13 London, W12 0BZ, UK

14

\*Correspondence to: Gang I. Chen (gang.chen@imperial.ac.uk)

### 16 Abstract

17

18

19

20

21

22

23

24

25

26

27

28

29

30

31

32

33

34

35

Particulate matter (PM) poses both health and climate risks. Understanding pollution sources is therefore crucial for effective mitigation. Positive Matrix Factorization (PMF) of Aerosol Chemical Speciation Monitor (ACSM) data is a powerful tool to quantify organic aerosol (OA) sources. A year-long study of ACSM data from London's Marylebone Road monitoring station during the COVID-19 pandemic provides insights into the impact of lockdown and the Eat Out To Help Out (EOTHO) scheme, which offered support to the hospitality industry during the pandemic, on PM composition and OA sources. Five OA sources were identified including hydrocarbon-like OA (HOA, traffic-related, 11% to OA), cooking OA (COA, 20%), biomass burning OA (BBOA, 12%), more-oxidized oxygenated OA (MO-OOA, 38%), and less-oxidized oxygenated OA (LO-OOA, 21%). Lockdown significantly reduced HOA (-52%), COA (-67%), and BBOA (-42%) compared to their pre-COVID levels, while EOTHO doubled COA (+100%) compared to the postlockdown period. However, MO-OOA and LO-OOA were less affected, as these primarily originated from long-range transport. This research has highlighted the importance of commercial cooking as a significant source of OA (20%) and PM<sub>1</sub> (9%) in urban areas. The co-emission of BBOA with COA observed in Central London demonstrates a similar diurnal cycle and response to the EOTHO policy, indicating that cooking activities might be currently underestimated and contribute to urban BBOA. Therefore, more effort is required to quantify this source and develop targeted abatement policies to mitigate emissions as currently limited regulation is in force.

### 1 Introduction

36

37

38

39

40

41

42

43

44

45

46

47

48

49

50

51

52

53

54

55

56

57

58

Atmospheric particulate matter (PM) are tiny particles suspended in the air, which can not only impact the climate directly and indirectly (IPCC, 2021; Seinfeld et al., 2006), but also cause adverse health effects to human (Kelly and Fussell, 2012; World Health Organization, 2021). PM consist of various constituents, including inorganic species (metals, minerals, black carbon, nitrate, sulphate, etc.) and organic species (complex mixture of thousands of compounds). European Environment Agency has reported that 99% of urban population in Europe are still exposed to polluted air with annual PM<sub>2.5</sub> (PM with aerodynamic diameter smaller than 2.5 µm) concentrations exceeding the WHO air quality guideline, 5 µg/m<sup>3</sup> (Europe's air quality status 2024, 2024; World Health Organization, 2021). As the most health-relevant air pollutant, PM<sub>2.5</sub> has shown strong associations with cardiovascular and respiratory related mortalities and hospital admissions (Dominici et al., 2006; Joo et al., 2024; Pye et al., 2021; Wei et al., 2022, 2024). Several studies have demonstrated that different constituents/sources contribute to health effects differently with varying toxicities (Daellenbach et al., 2020; Kelly and Fussell, 2012; Liu et al., 2023; Vasilakopoulou et al., 2023). Therefore, targeting the specific composition/sources of PM that are most health-relevant could be the most cost-effective way to mitigate its adverse health effects. Click or tap here to enter text. Coronavirus disease 19 (COVID-19) started to spread rapidly worldwide since the first case was identified in Wuhan, China late in 2019. Many countries implemented measures to contain COVID cases, which significantly restricted social and economic activities. In the UK, starting from the end of Mar 26th, 2020, people were ordered to stay at home and all non-essential businesses were closed, including pubs, cafes and restaurants. Non-essential shops were allowed to open on Jun 15<sup>th</sup>, and the first national lockdown came to an

end Jun 23<sup>rd</sup>, 2020. However, pubs, restaurants, and cafes were only allowed to open from July 4<sup>th</sup>. 59 60 2020. Subsequently, the Eat Out to Help Out (EOTHO) Scheme was designed to help the 61 hospitality industry; offering a 50% meal discount up to a maximum of £10 and operated Monday to Wednesday during from Aug 3<sup>rd</sup> to Aug 31<sup>st</sup>, 2020; https://www.gov.uk/guidance/get-a-62 63 discount-with-the-eat-out-to-help-out-scheme. 64 The UK recorded a 2.5% drop in Gross Domestic Product (GDP) in the first quarter of 2020, partly 65 as people reduced their own activity prior to the legally enforced lockdown measures introduced 66 on Mar 26<sup>th</sup>. This accelerated to a 19.8% fall in GDP in April to June 2020 and household spending 67 fell by over 20% over this period, the largest quarterly contraction on record, which was driven by 68 falls in spending on restaurants, hotels, transport, and recreation (ONS, 2022). 69 Some studies have investigated the lockdown impacts on chemical composition and sources of 70 PM, which mainly focused on cities in China (Hu et al., 2022; Tian et al., 2021; Xu et al., 2020), 71 a kerbside site in Toronto, Canada (Jeong et al., 2022), and an urban background site in Paris, 72 France (Petit et al., 2021). These studies all resolved primary sources including traffic related 73 emissions, biomass burning emissions from residential heating, cooking emissions (except Paris), 74 and secondary sources from PMF analysis on organic aerosol (OA). Traffic and cooking emissions 75 appeared to decrease during the lockdown in all sites, while biomass burning predominately from 76 residential heating sources in Chinese cities increased as result of remote work and rather early 77 lockdown measures (Jan-Feb 2020) compared to France. Secondary organic aerosol (SOA) 78 showed a more complex phenomenon given its abundance in organic components and dynamic 79 spatiotemporal conditions. Overall, the lockdowns resulted in decreased SOA in both northwest 80 cities in China (Tian et al., 2021; Xu et al., 2020) and Paris (Petit et al., 2021) due to lower primary 81 emissions, and therefore fewer SOA formation products. However, Beijing experienced a large

increase in SOA concentrations due to increased fossil fuel and biomass emissions, long-range transport influences as well as favourable meteorological conditions (high RH, low wind speed and low boundary layer height) for SOA formation during the lockdown period (Hu et al., 2022). Therefore, the lockdown effects on the SOA were dependent on the abundance of primary emissions, long-range transported air masses, and meteorological conditions. To date, there are few studies that investigate how COVID-related policies could have impacted PM chemical composition and sources. Petit et al. (2021) and Gamelas et al., (2023) are only two studies in Europe. The unique COVID-related policies in the UK provided a rare opportunity to investigate the impacts these policies had on chemical composition and OA sources. To address these issues, we used highly time resolved measurements from an air quality supersite located in the Central London from 2019 to 2020, and advanced source apportionment approaches to quantify the influence of the first lockdown and EOTHO scheme on the PM composition and OA sources. This provides unique insight into PM sources and composition in a global mega city.

## 2 Methodology

#### 96 2.1 Air quality monitoring supersite in central London

The London Marylebone Road supersite (MY, 51.52 N, -0.15 E) is a kerbside monitoring site, one meter away from a busy 6-lane road in central London. It is a well-established air quality supersite that has consistently generated high-quality air pollution data since 1997 including mass concentration of bulk PM<sub>1</sub>, PM<sub>2.5</sub>, and PM<sub>10</sub>, as well as PM composition including black carbon, heavy metals, nitrate (NO<sub>3</sub>), sulphate (SO<sub>4</sub>), ammonium (NH<sub>4</sub>), OA, Chloride (Cl), etc. More details of this site can be found at https://uk-air.defra.gov.uk/networks/site-info?site\_id=MY1.

#### 2.2 Instrumentations

103

104

105

106

107

108

109

110

111

112

113

114

115

116

117

118

119

120

121

122

123

124

Quadrupole ACSM (Q-ACSM, Aerodyne, Ltd., Ng et al. (2011)) with a standard vaporizer provides 30-min mass loadings of chemical species within non-refractory submicron aerosol (NR-PM<sub>1</sub>), including NH<sub>4</sub>, NO<sub>3</sub>, SO<sub>4</sub>, Cl, and OA. Sampled particles are focused into a narrow beam using the aerodynamic lens and impacted on a filament surface at 600 °C, where the NR-PM<sub>1</sub> is vaporised and ionised instantly by an electron impact source (70eV). These ions are detected by the RGA quadrupole mass spectroscopy to provide a mass spectrum of NR-PM<sub>1</sub> up to a mass-tocharge ratio (m/z) of 148 Th. The mass concentration of different chemical species are calculated using the fragmentation table developed by Allan et al. (2004), updated for Cl following suggestions provided by Tobler et al. (2020), and a composition-dependent collection efficiency (CDCE) correction suggested by Middlebrook et al. (2012) by following the ACTRIS standard operation procedure (https://www.actris-ecac.eu/pmc-non-refractory-organics-and-inorganics). With co-located black carbon (BC) measurement using a PM<sub>2.5</sub> cyclone with AE33 (Aerosol Magee Scientific, Ltd.) and PM<sub>1</sub> measurements using FIDAS (Palas, GmbH), we conducted the mass closure for fine particles measurements. The sum of NR-PM<sub>1</sub> and BC (in PM<sub>2.5</sub>) reproduces PM<sub>1</sub> concentrations well, with a slope of 1.13 and an R<sup>2</sup> of 0.73 (Fig. S1).

### 2.3 Sampling periods and COVID-related policies

PM<sub>1</sub> chemical composition from Aug 1<sup>st</sup>, 2019 to Oct 22<sup>nd</sup>, 2020, was analysed as this covered the first lockdown period (Mar 26<sup>th</sup>–23 Jun 23<sup>rd</sup>, 2020) and the EOTHO Scheme (Mon-Wed during from Aug 3<sup>rd</sup> to Aug 31<sup>st</sup>, 2020, Table 1). In order to isolate the seasonal effects on the PM chemical composition and OA sources from the COVID-related policies, we further split the data based on seasons (Table 1). In addition, deweathering analysis has been conducted using "worldmet" R

package (Carslaw, 2025) to remove the meteorological effects (i.e., relative humidity, wind speed, wind direction, and air temperature) on all PM/OA species as shown in the SI (Fig. S8 and Fig. S9). Meteorological effects were considerable, especially for Pre-lockdown Spring period, while it does not change the conclusion of the effects from lockdown and EOTHO policies. Therefore, the main results presented in this study are based on the original measurements.

Table 1 Dates of the COVID-related policies in London

COVID Policies		Date
Pre-Lockdown	Summer	Aug 1st-Aug 31st, 2019
	Fall	Sep 1 <sup>st</sup> –Nov 30 <sup>th</sup> , 2019
	Winter	Dec 1st, 2019–Feb 28th, 2019
	Spring	Mar 1 <sup>st</sup> –Mar 25 <sup>th</sup> , 2020
Lockdown	Spring	Mar 26 <sup>th</sup> –May 31 <sup>st</sup> , 2020
	Summer	Jun 1 <sup>st</sup> –Jun 23 <sup>rd</sup> , 2020
Post-Lockdown	Pre-EOTHO	Jun 24 <sup>th</sup> -Aug 2 <sup>nd</sup> , 2020
	ЕОТНО	Aug 3 <sup>rd</sup> –Aug 31 <sup>st</sup> , 2020
	Post-EOTHO	Sep 1 <sup>st</sup> –Oct 22 <sup>nd</sup> , 2020

#### 2.4 Source apportionment

Source apportionment is a common but powerful approach to identifying and quantifying the emission sources and atmospheric constituents of PM based on measurements. As the sources of inorganic species (black carbon, ammonium, nitrate, chloride, sulphate, etc.) are relatively well-studied, most of the studies are focused on deconvoluting the sources of OA, which contains thousands of compounds. Positive matrix factorization (PMF) is one of the receptor models that is

138 widely utilized in the field to conduct source apportionment analysis (Jimenez et al., 2009; Zhang 139 et al., 2007). Typically, an Aerodyne aerosol mass spectrometer (AMS, Aerodyne Ltd., USA, 140 Jayne et al., 2000) is used to measure the time series of both inorganic and organic species of non-141 refractory PM, in which, organic mass spectra are used for PMF analysis. However, operating an 142 AMS is labour-intense and expensive. In contrast, the aerosol chemical speciation monitor (ACSM, 143 Aerodyne, Ltd., Fröhlich et al., 2013; Ng et al., 2011) has been designed for long-term monitoring 144 purposes with less maintenance and lower capital cost, which has gained popularity across Europe 145 (Chebaicheb et al., 2024; Chen et al., 2022; Laj et al., 2024) and the U.S. 146 (https://ascent.research.gatech.edu/, Hass-Mitchell et al., 2024; Joo et al., 2024). Chen et al. (2022) 147 demonstrated a robust protocol to conduct advanced PMF analysis on long-term ACSM datasets, 148 which delivers high-quality and consistent source apportionment results. This study follows this 149 standardized protocol to resolve the OA sources in London by implementing advanced PMF 150 techniques. 151 Advanced source apportionment approaches have been used in this study, including rolling 152 positive matrix factorization (PMF), ME-2 with random a-value approach, bootstrap and criteria-153 based selections (Canonaco et al., 2021; Chen et al., 2022). The standardized protocol of rolling 154 PMF as presented in Chen et al. (2022) was used to ensure high-quality and comparable sources 155 of OA were retrieved in London. Specifically, PMF was first done on four different seasons as 156 suggested in Chen et al. (2022) to determine the optimum number of factors. A total of 5 OA 157 factors were identified: hydrocarbon-like OA (HOA), cooking-like OA (COA), biomass burning 158 OA (BBOA), more-oxidized OOA (MO-OOA) and less-oxidized OOA (LO-OOA). Adding an 159 additional factor resulted in split of COA factor, decreasing it to four factors caused mixing 160 between the MO-OOA and COA factors. Therefore, 5 factor-solution was determined across the

162

163

164

165

166

167

168

169

170

171

172

173

174

175

176

177

178

179

180

181

182

whole year. In addition, site-specific factor profiles were derived for HOA, COA, and BBOA through a seasonal bootstrap PMF analysis for winter (Dec, Jan, and Feb) and used as constraints as suggested in Chen et al. (2022) and Via et al. (2022). However, the MY site is surrounded by many restaurants with prevalent cooking emissions. Thus, the chemical fingerprint for both HOA and COA might not be fully separated. Therefore, we constrained the trend of NO<sub>x</sub> time series, BBOA and COA profiles from a previous winter bootstrap solution collected in London North Kensington (2015-2018, Chen et al., 2022) to retrieve environmentally reasonable results with five factors in winter data, so-called base case solution. Then, a bootstrap resampling analysis with 100 iterations and five factors was conducted by constraining the factor profiles of HOA, COA, and BBOA from the base case with random a-value from 0.1-0.5 with step of 0.1. It results in stable factor profiles of these three primary sources as shown in Fig. S2, which shows good agreements with published reference profiles (Chen et al., 2022; Crippa et al., 2013). Rolling PMF was conducted with a time window of 14 days and a step of 1 day by constraining primary factor profiles of HOA, COA, BBOA in Fig. S2 (averaged bootstrap results) and two additional unconstrained factors with bootstrap resampling and the random a-value option (0.1-0.5, step of 0.1, 50 iterations/window). A criteria list including selections based on both time series and factor profiles as shown in Table S1 was applied as per Chen et al. (2022). With the help of ttest in temporal-based criteria (1-3), we can minimize subjective judgements in determining the environmentally reasonable results. Eventually, 3,166 runs (14.1%) of the PMF runs were selected across different rolling windows across the whole year to average as the final results (utilized avalues were averaged to two decimal places) with 4.9 % unmodelled data points, which is comparable with other rolling PMF analyses (Chen et al., 2022).

### 3 Results and Discussions

3.1 Chemical composition of submicron PM for different periods around the

COVID-19 Lockdown

183

184

185

186

187

188

189

190

191

192

193

194

195

196

197

198

199

200

201

202

The average PM<sub>1</sub> mass concentration at MY site was 11 µg/m<sup>3</sup> for the study period with 44% OA, 21% NO<sub>3</sub>, 15% SO<sub>4</sub>, 16% BC, 5% NH<sub>4</sub>, and 0.6% Cl. The distribution of the chemical composition on PM<sub>1</sub> varied depending on the season and variation was associated with the lockdown and EOTHO policies (Figure 1). PM<sub>1</sub> increased by 95% in lockdown spring (Mar 26<sup>th</sup>–May 31<sup>st</sup>, 2020) compared to pre-lockdown spring (Mar 1<sup>st</sup>–Mar 25<sup>th</sup>, 2020). Specifically, Org, SO<sub>4</sub>, NO<sub>3</sub>, NH<sub>4</sub>, and Cl all increased by 87%, 211%, 73%, 237%, and 132%, respectively. Except for BC, which decreased by 52%. This is due to the polluted airmass originating from mainland Europe and the enhanced agricultural emissions in spring from the UK and wider continental Europe (Aksoyoglu et al., 2020). It was further confirmed, through back trajectory analysis, that elevated PM<sub>1</sub> events (Mar 25<sup>th</sup>–Mar 28<sup>th</sup>, Apr 8<sup>th</sup>–Apr 10<sup>th</sup>, and Apr 15<sup>th</sup>–Apr 17<sup>th</sup>), where the result of airmasses passing over northern continental Europe (Fig. S6). In addition, the Org, SO<sub>4</sub>, NO<sub>3</sub>, NH<sub>4</sub>, and Cl were only increased by 21%, 107%, 50%, and 28% respectively after the deweathering analysis (Fig. S8), suggesting significant meteorological influences during this period. NO<sub>3</sub> concentration reduced in summer 2019 and 2020 as expected compared to spring or fall seasons due to the volatility of NH<sub>4</sub>NO<sub>3</sub> and lower agricultural emissions, while SO<sub>4</sub> concentrations increased in summer due to enhanced photochemistry (Bressi et al., 2021; Chen et al., 2022). During the lockdown in spring SO<sub>4</sub> concentrations remained high, which was associated with long-range transport (Fig. S7).

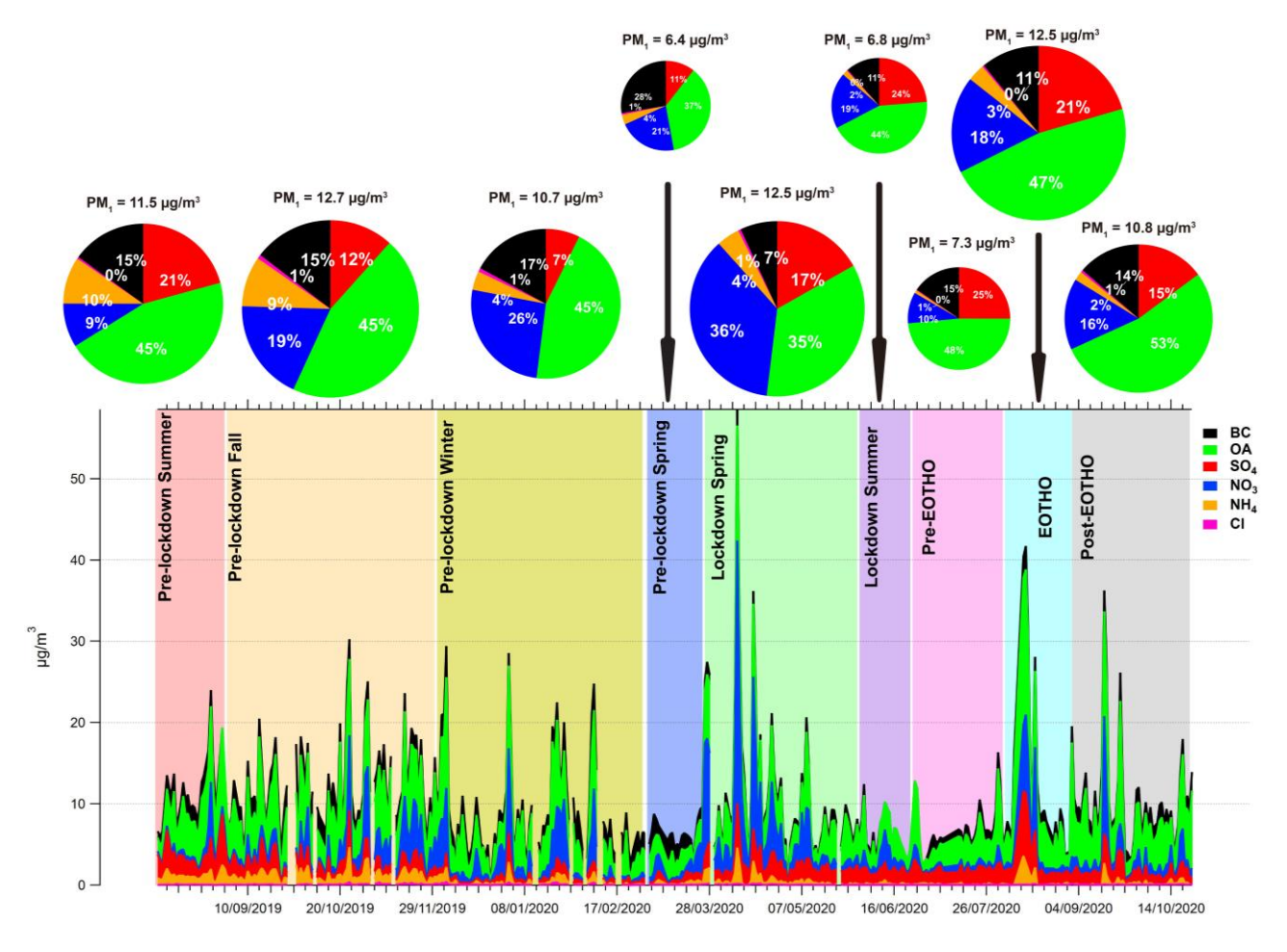


Figure 1 Chemical compositions of PM<sub>1</sub> at MY from Aug 2019 to Oct 2020 (daily resolution) and averaged for the different periods as shown in Table 1.

BC concentrations during the spring lockdown (Mar 26<sup>th</sup>–May 31<sup>st</sup> 2020) reduced from 1.78 to 0.86 μg/m³ (-52%) compared to the pre-lockdown level in spring (Mar 1<sup>st</sup>–Mar 25<sup>th</sup>), due to the significant reduction in traffic during the first lockdown (Transport for London, 2020). Similar decreasing of BC has been observed elsewhere during COVID lockdown as described in introduction (Gamelas et al., 2023; Jeong et al., 2022; Petit et al., 2021; Tian et al., 2021; Xu et al., 2020). It is worth noting that the BC concentration had already reduced by 3% in pre-lockdown spring (Mar 1<sup>st</sup>–Mar 25<sup>th</sup>) compared to the pre-lockdown winter. This is likely due to vehicle mileage reducing as the UK government implemented travel restrictions and advised people to work from home on Mar 16<sup>th</sup>, 2020 (Transport for London, 2020). BC increased to 1.13 μg/m³

(+44%) after the lockdown and before the EOTHO (Jun 24<sup>th</sup>–Aug 2<sup>nd</sup>,2020, pre-EOTHO in Figure 1) as people returned to work and travel. However, BC concentrations remained 34% lower than the pre-lockdown summer (Aug 1<sup>st</sup>–Aug 31<sup>st</sup>, 2019) concentration of 1.72 μg/m³ (Fig. S9), which suggests that the traffic emissions reduced considerably as the fewer economic activities even after the ease of the first lockdown (e.g., suggestions of hybrid working mode, restricted international travel, reduced tourism, limited access to entertainments). BC also increased to 1.35 μg/m³ (+19%) during the EOTHO scheme (Aug 3<sup>rd</sup>–Aug 31<sup>st</sup>, 2020). This was not only because of increased traffic emission during this period, but may also result from cooking activities (e,g, barbecuing or wood-fired cooking styles) in Central London (Defra, 2023). Since the EOTHO was only in place from Mon to Wed, BC concentrations (likely due to increased traffic and cooking emissions) increased on Mon-Wed compared to post-lockdown but before EOTHO (Jun 24<sup>th</sup>–Aug 2<sup>nd</sup>, 2020) (Fig. S10).

#### 227 3.2 OA sources in Central London

As mentioned above, the rolling PMF analysis resolved 5 factor solutions, including HOA, COA, BBOA, MO-OOA, and LO-OOA as shown in Figure 3 and Figure 4. The left panel of Figure 3 shows the yearly averaged factor profiles of resolved PMF factors and total OOA calculated as the sum of LO-OOA and MO-OOA. All factors show good agreements with previous studies in terms of key m/z tracers. In addition, as shown in Figure 2, tError! Reference source not found.he contribution to total OA concentrations from HOA, BBOA, and LO-OOA was consistent at different OA concentrations. However, the contribution of COA increased as total OA concentrations increased. This suggests that cooking emissions in Central London are responsible for elevated OA concentrations, which was also the case in Athens as shown in Chen et al. (2022).

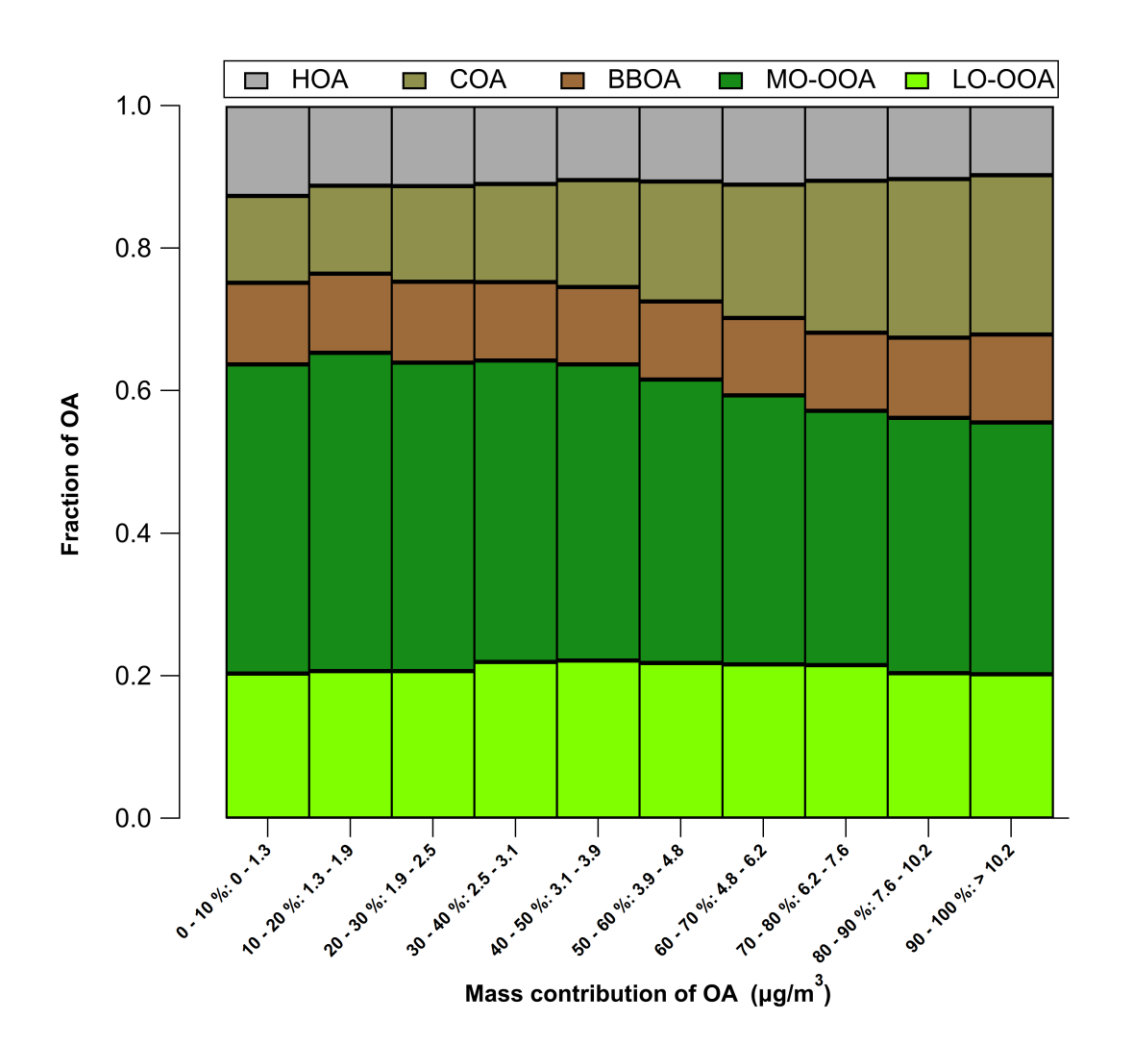


Figure 2 Contributions to total OA from the different identified OA sources at different OA concentrations. Total OA concentrations were split in 10 equally distributed bins.

#### 3.2.1 General characteristics of OA factors

 $\begin{array}{c} 238 \\ 239 \end{array}$ 

The right panel of Figure 3 shows time series (daily averaged) and Figure 4 shows diurnal cycles for each OA factor. The mean concentrations of HOA, COA, BBOA, MO-OOA, LO-OOA, and OOA (MO-OOA+LO-OOA) were  $0.50 \pm 0.1~\mu g/m^3$ ,  $0.93 \pm 0.14~\mu g/m^3$ ,  $0.55 \pm 0.11~\mu g/m^3$ ,  $1.81 \pm 0.41~\mu g/m^3$ ,  $1.00 \pm 0.44~\mu g/m^3$ , and  $2.80 \pm 0.70~\mu g/m^3$ , and contributed to OA (PM<sub>1</sub>) with the fractions of 11% (5% to PM<sub>1</sub>), 20% (9% to PM<sub>1</sub>), 12% (5% to PM<sub>1</sub>), 38% (17% to PM<sub>1</sub>), 21% (9% to PM<sub>1</sub>), and 59% (26% to PM<sub>1</sub>), respectively. The concentration of all OA factors shows strong time variations over the year as shown on the Figure 4. OA factors also showed considerable

seasonality besides the effects from COVID-related policies (Figure 4 and Fig. S3). POA concentrations were generally lower in the warmer seasons than in winter as lower temperature favours particle formation via condensation and dilution and dispersion are reduced due to the lower boundary layer. It's worth mentioning that the reduced POA concentrations in warm season was not caused by reduced residential heating and energy consummation since Central London mainly uses natural gas and renewable energy instead of solid fuel combustions. The OOA factor concentrations remain relatively consistent across seasons, while its contributions were larger during the warmer seasons (Fig. S4). This is because both high temperature and strong irradiation will enhance the photochemistry and evaporation of POA sources and the increased biogenic volatile organic compound (VOC) emissions lead to high OOA production despite the evaporation of semi-volatile OOA (Fig. S4). The temporal variations observed here in central London was consistent with the other urban sites across Europe (Chen et al., 2022). Therefore, this study focuses on the impacts of COVID-related polices on OA sources.

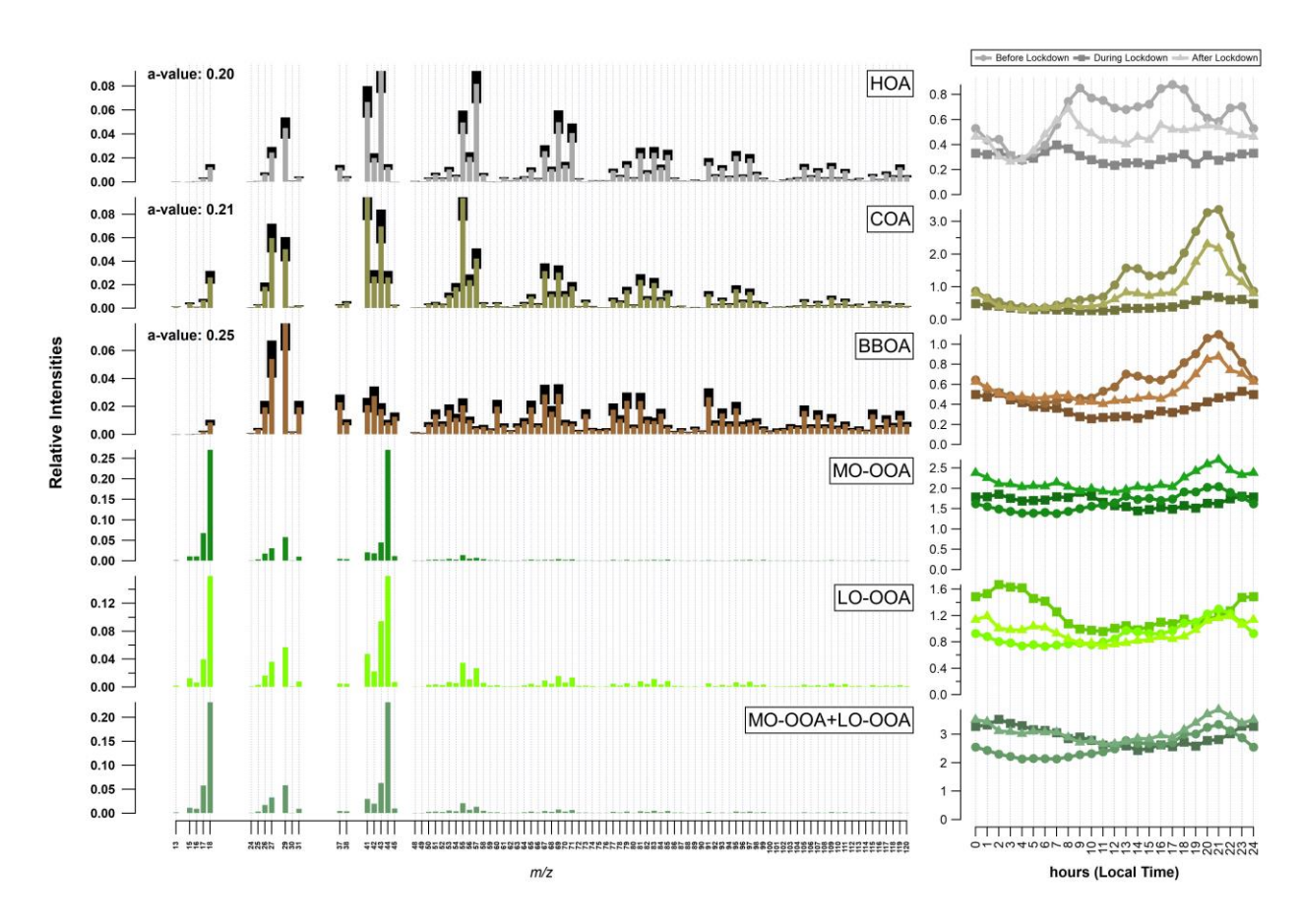


Figure 3 Yearly averaged profiles (left) and diurnal cycles (right) of resolved factors from the rolling PMF analysis at the MY site. Time is expressed in local time.

 $\begin{array}{c} 262 \\ 263 \end{array}$ 

The right side of Figure 3 shows the diurnal cycles before, during, and after the lockdown. POA factors showed distinct diurnal variations, in which HOA showed morning and evening rush hour peaks, COA showed distinct lunchtime and evening peaks, and BBOA showed a similar pattern as COA before and after the lockdown. This indicates that the part of what is measured as BBOA in central London is most likely co-emitted from cooking activity, most likely from barbecuing style or wood-oven pizza restaurants in the area. A survey about use of domestic fuels in the hospitality sector was conducted by Department for Environment Food and Rural Affairs (Defra), UK suggested that restaurants use solid fuel to cook to provide unique flavours (Defra, 2023). Mohr et al. (2009) showed that meat-cooking can slightly elevate m/z 60, which is an important ion in the BBOA factor profile. OOA factors showed much less diurnal variation compared to

POA factors in all periods, this is in agreement with the other 22 European sites reported in Chen et al. (2022). The MO-OOA showed a smaller diurnal variation compared to LO-OOA.

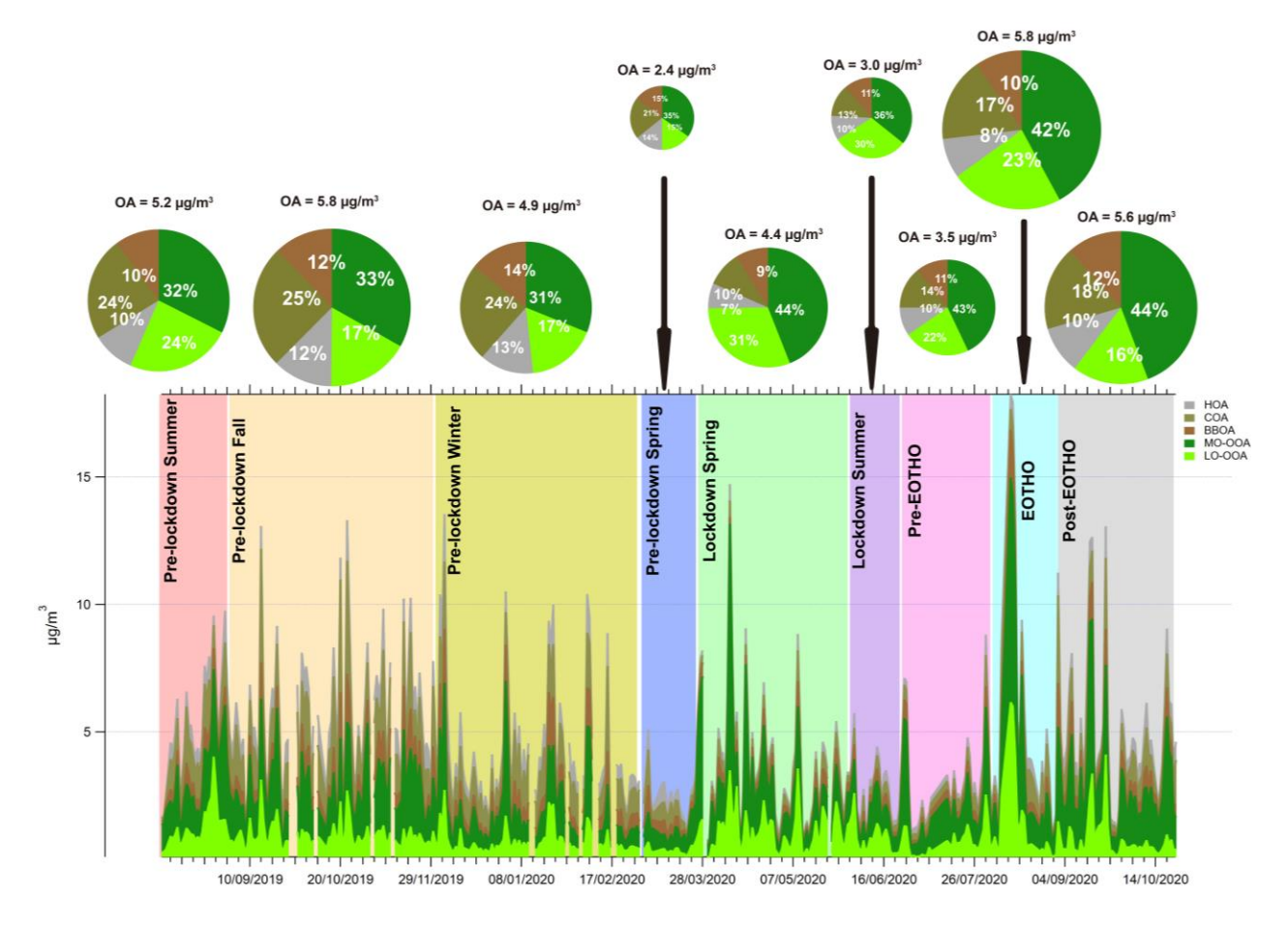


Figure 4 Average mass concentrations for OA sources at MY during different periods from Aug 2019 to Oct 2020

### 3.2.2 <u>Pre-lockdown Spring Pre-lockdown Spring</u>

In general, OA concentration decreased by 51% in pre-lockdown spring compared to pre-lockdown winter (Dec 1<sup>st</sup>, 2019–Feb 28<sup>th</sup>, 2020) due to seasonality, origins of airmass (Fig. S5), and the impact of lockdown. OOA concentrations also decreased drastically by 50%. Primary emissions were significantly lower due to reduced vehicle mileage and other economic activity before the official lockdown measure came into force on March 26<sup>th</sup> 2020 (Figure 3 (a) and Figure 4) as suggested by the 1<sup>st</sup> quarter drop in GDP (ONS, 2022). Atmospheric components related to vehicle emissions (HOA and BC) decreased by 48% and 3% respectively, in early March 2020.

COA decreased by 58% due to fewer restaurant activity, BBOA decreased by 50% was likely due to the reduced commercial cooking using charcoal and wood as well as warmer weather requiring less domestic space heating.

#### 3.2.3 Lockdown

286

287

288

289

290

291

292

293

294

295

296

297

298

299

300

301

302

303

304

305

306

307

308

The diurnal variation of COA and BBOA during lockdown showed much less intensity overall but the distinctive lunchtime peak remained as the pre-lockdown; and the evening peak reduced its intensity (Figure 3). HOA retained distinct morning and evening rush hour peaks but at lower mass concentrations during lockdown (Figure 3). This is because the takeout activities of some restaurants were still active as well as the potential increases for residential cooking activities during lockdown. After the first lockdown, the distinct lunch and evening peaks in diurnal patterns of COA and BBOA reappeared as the open-up of nearby restaurants. The morning and evening rush hour peaks for HOA enhanced considerably as the ease of the travel restrictions after the first lockdown. However, POA concentrations did not reach pre-COVID levels (Fig. 5). This is likely due to widespread hybrid working and the remaining oversea travel restrictions supressing tourism, which reduced traffic activity and restaurants visits. Conversely, OOA concentrations during lockdown were slightly higher than pre-lockdown levels. These were related to long-range transport, with relatively high mass concentrations of MO-OOA and LO-OOA during the lockdown (Fig. S5 and Fig. S6). Compared to the pre-lockdown spring, HOA and COA in the lockdown spring decreased by 11% and 15%, respectively, while BBOA increased marginally by 13% (from 0.35 to 0.39  $\mu$ g/m<sup>3</sup>) (Figure 5). MO-OOA and LO-OOA increased by 136% and 279%, respectively due to long-range transportation of airmasses from continental Europe (Fig. S5 and Fig. S6) and increased photochemistry (enhanced temperature and ozone levels in Fig. S4) compared to the first 25 days in Mar 2020. This was accompanied by increased SO<sub>4</sub> (+211%), NH<sub>4</sub>

(+132%) and NO<sub>3</sub> (+237%) as shown in Fig. S9, despite the higher temperature could favour partitioning these species into the gas phase.

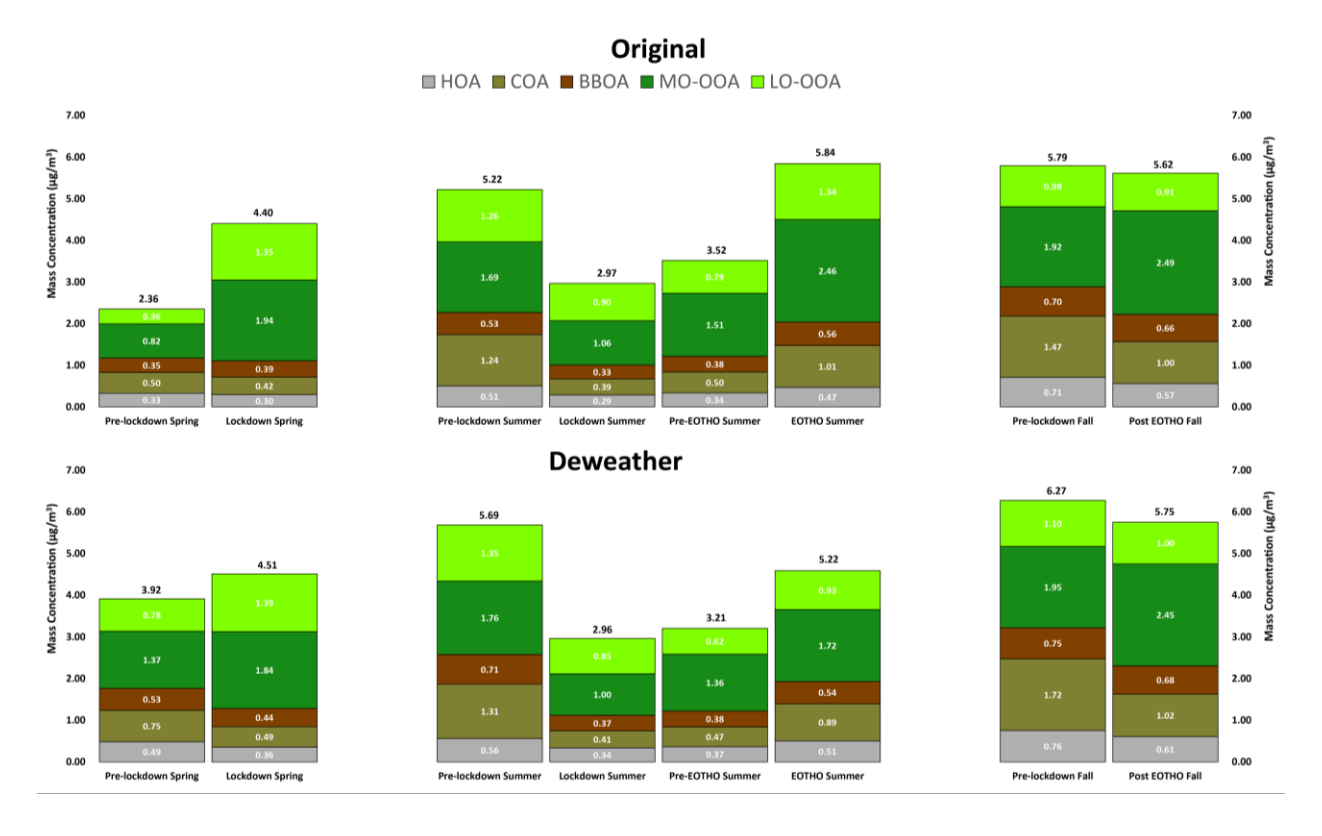


Figure 5 The impacts on OA sources during different periods compared with business-as-usual cases with and without deweathering analysis.

In June 2020, still in lockdown (Jun 1<sup>st</sup>– Jun 23<sup>rd</sup>, 2020), POA showed further but marginal decreases (-3%, -8%, and -15% for HOA, COA, and BBOA, respectively, Figure 4) compared to the lockdown spring as the enhanced photochemistry leads to increased formation of OOA from the POA. However, the overall mass concentration of MO-OOA and LO-OOA decreased significantly by 45%, and 34%, respectively as the result of fewer long-range transported airmasses (Fig. S5).

During pre-EOTHO (Jun 24<sup>th</sup>–Aug 2<sup>nd</sup>, 2020), HOA, COA, and BBOA all showed considerably increases of 16%, 30%, and 14%, respectively when compared to lockdown summer period. In which, MO-OOA increased by 45% and LO-OOA decreased by 13%, respectively as the relatively

higher temperature and irradiations were favouring the vaporization of LO-OOA and production of MO-OOA from LO-OOA and POA. As shown in Figure 5, the POA concentrations were much lower when compared to summer 2019 (Aug 1<sup>st</sup>–Aug 31<sup>st</sup>, 2019) as travel and economic activities did not return to pre-COVID levels (ONS, 2022; Transport for London, 2020). Specifically, reduced vehicle mileage resulted in lower HOA (-33%), BC (-37%), COA (-59%) due to the reduced commercial cooking activity. As BBOA is co-emitted with COA during of cooking activities, BBOA also decreased slightly from 0.53 to 0.38 μg/m³ (-28%, Figure 5).

#### 3.2.4 Eat Out To Help Out (EOTHO)

EOTHO policy (Aug 3<sup>rd</sup>–Aug 31<sup>st</sup>, 2020) had a significant impact on all POA factors. In particular, the COA concentration increased by 100% compared to the post-lockdown period (Pre-EOTHO Summer) from Jun 24<sup>th</sup> to Aug 2<sup>nd</sup>, 2020 (0.5 to 1.0 μg/m³, Figure 6). HOA and BBOA concentrations also increased by 40% and 48%, respectively, which suggested the human activities resulting in these emissions recovered slowly after the lockdown (ONS, 2022; Transport for London, 2020). COA was significantly higher due to EOTHO, however, it did not reach pre-COVID concentrations (Figure 5 and Figure 6) as its level was lower on each weekday except for Mon.

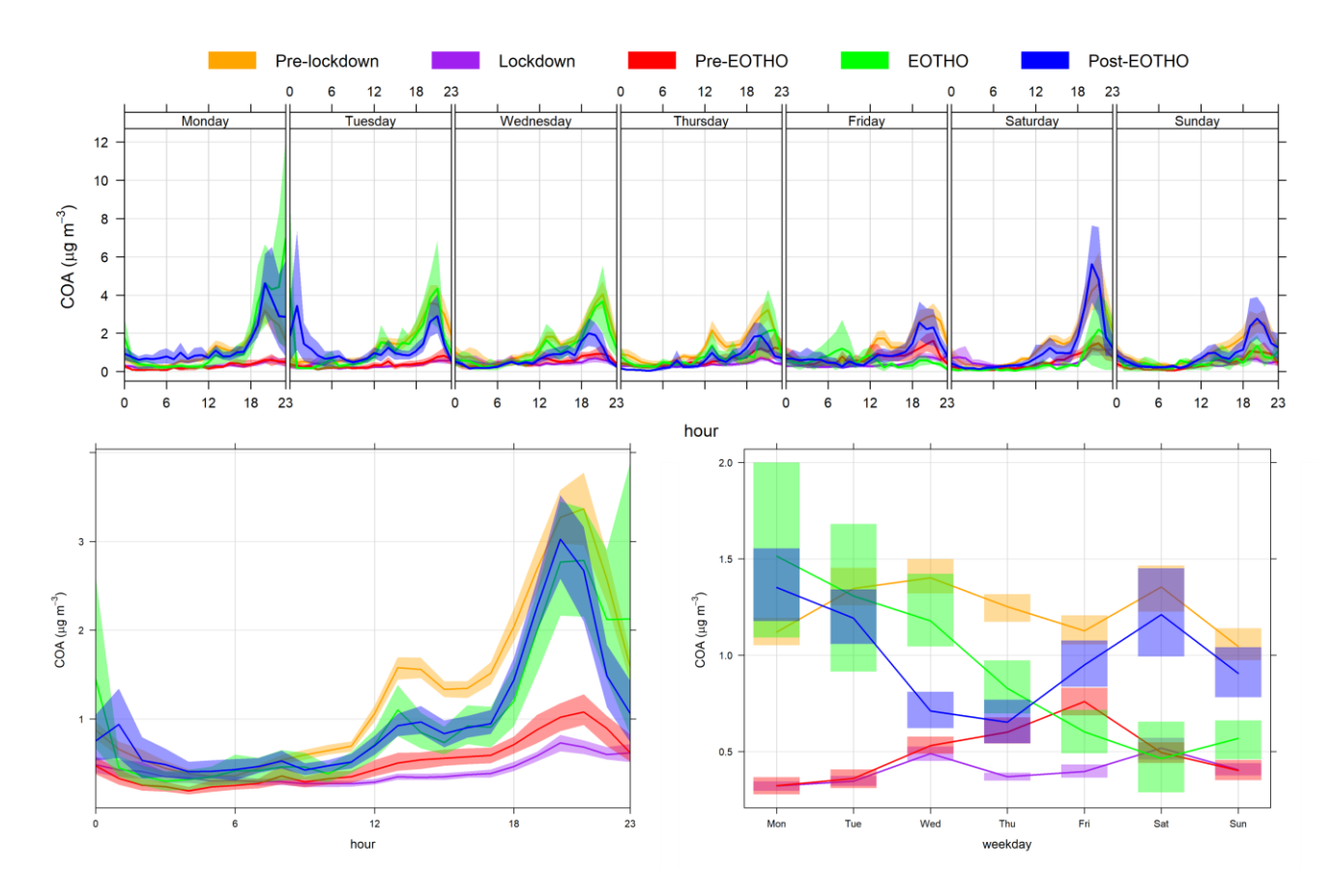


Figure 6 . COA diurnal plots for each weekday, diurnal plots, and weekly plots at different periods in relation with COVIDrelated policies

EOTHO only operated from Mon to Wed, and this was clear in the diurnal plots (Figure 6 and Fig. S12) with larger COA concentrations from Mon to Wed, in contrast with larger concentrations over the weekend (Fri to Sun) before EOTHO (Jun 24<sup>th</sup>–Aug 2<sup>nd</sup>, 2020). Interestingly, even after the EOTHO policy ceased (Sep 1<sup>st</sup>–Oct 22<sup>nd</sup>, 2020), COA levels remained elevated on Mon and Tue but a much higher level during the weekend was observed. This suggests that EOTHO had an influence on the consumer behaviour even after the lockdown. It is also worth noting that the high concentrations of COA and BBOA (Figure 6 and Fig. S11) on Monday night were caused by the last day of EOTHO policy coinciding with a UK public holiday on Aug 31<sup>st</sup>.

Also, during EOTHO, MO-OOA and LO-OOA increased by 63% and 70% respectively compared

to post-lockdown concentrations before EOTHO and correlated with increased NH<sub>4</sub>, NO<sub>3</sub> and SO<sub>4</sub>

concentrations. This was mainly due to long-ranged transported airmasses (Fig. S5) and enhanced photochemistry with increased temperature and mass concentration of POAs (Fig. S4).

### 4 Conclusion

352

353

354

355

356

357

358

359

360

361

362

363

364

365

366

367

368

369

370

371

372

373

This study demonstrates the importance of source apportionment studies to better understand how national and local government policies can impact the PM mixture, and how these effects can be differentiated from the influences of meteorology and large-scale atmospheric processes. PM concentrations increased at the beginning of the lockdown (Mar-Apr 2020) despite reduced economic activities, which was caused by long-range transported airmasses instead of primary emissions. Through examining the source apportionment (and inorganic PM composition), COVID-related policies were found to have profound but largely unintended impacts on air quality. The first lockdown significantly reduced POA sources: including HOA by 52%, COA by 67%, and BBOA by 42%. While all these components reduced dramatically during the lockdown, they only gradually increased again and did not reach pre-COVID levels during the duration of this study (Aug 2019-Oct 2020). Most significantly, while the Eat Out To Help Out (EOTHO) policy was effective in helping the hospitality industry to recover from economic losses during the lockdown, it had unintended impacts on air quality as cooking emissions increased. Clearly detecting this change confirms the presence of COA (20% to OA) as an important source of OA in London and the importance of commercial cooking as a source. Also of note was the impact that EOTHO had on BBOA concentrations, which increased by 48% while this policy was in place. This establishes a clear link between commercial cooking activity and BBOA measured in cities due to the use of charcoal and wood as cooking fuels (Defra, 2023), as well as potentially emissions from cooking ingredients. Cooking may therefore be underestimated as a source if COA concentrations are considered in isolation, and BBOA is only associated with other sources of solid fuel burning. This emphasises the need to develop policies and technical solutions to mitigate commercial cooking emissions in the urban environment, especially as there are limited regulations on this industry in terms of air pollution. There are filter technologies (e.g., electrostatic precipitators, UV-C lamp exhaust hood, hydrovents) available that have been implemented as law in Hong Kong to effectively control cooking emissions (Hong Kong EPD, 2024). It also demonstrated the importance in continuous monitoring with subsequent source apportionment analysis to better understand the influence of government policies to improve air quality more effectively.

## Code/Data availability

Rolling PMF analyses is run using SoFi Pro from Datalystica (https://datalystica.com/sofi-pro/, Datalystica, 2024) under Igor Pro 9 platform from WaveMetrics® (https://www.wavemetrics.com/, WaveMetrics, 2024) and they are both available for purchase. Raw data/results from the study are available upon request to the corresponding author Gang I. Chen (gang.chen@imperial.ac.uk).

### Author contribution

Gang I. Chen: Writing – review & editing, Writing – original draft, Visualization, Validation, Project administration, Methodology, Investigation, Funding acquisition, Formal analysis, Data curation, Conceptualization. Anja H. Tremper: Writing – review & editing, Methodology, Formal analysis, Data curation. Max Priestman: Methodology, Formal analysis, Data curation. Anna Font: Writing – review & editing, Methodology, Formal analysis, Data curation. David C. Green: Writing – review & editing, Supervision, Project administration, Methodology, Resources, Funding acquisition, Conceptualization.

## Competing interests

The authors declare that they have no known competing financial interests or personal relationships that could have appeared to influence the work reported in this paper.

## Acknowledgement

This study is part funded by the National Institute for Health Research (NIHR) Health Protection Research Unit in Environmental Exposures and Health, a partnership between UK Health Security Agency (UKHSA) and Imperial College London. The views expressed are those of the authors and not necessarily those of the NIHR, UKHSA or the Department of Health and Social Care. This study was also supported by NERC Awards (NE/1007806/1)

### References

- 408 Aksoyoglu, S., Jiang, J., Ciarelli, G., Baltensperger, U., and Prévôt, A. S. H.: Role of ammonia in
- European air quality with changing land and ship emissions between 1990 and 2030, Atmos Chem
- 410 Phys, 20, 15665–15680, https://doi.org/10.5194/acp-20-15665-2020, 2020.
- 411 Allan, J. D., Delia, A. E., Coe, H., Bower, K. N., Alfarra, M. R., Jimenez, J. L., Middlebrook, A.
- 412 M., Drewnick, F., Onasch, T. B., Canagaratna, M. R., Jayne, J. T., and Worsnop, D. R.: A
- 413 generalised method for the extraction of chemically resolved mass spectra from Aerodyne aerosol
- 414 mass spectrometer data, J Aerosol Sci, 35, 909–922, https://doi.org/10.1016/j.jaerosci.2004.02.007,
- 415 2004.

407

- Bressi, M., Cavalli, F., Putaud, J. P., Fröhlich, R., Petit, J. E., Aas, W., Äijälä, M., Alastuey, A.,
- 417 Allan, J. D., Aurela, M., Berico, M., Bougiatioti, A., Bukowiecki, N., Canonaco, F., Crenn, V.,
- Dusanter, S., Ehn, M., Elsasser, M., Flentje, H., Graf, P., Green, D. C., Heikkinen, L., Hermann,
- 419 H., Holzinger, R., Hueglin, C., Keernik, H., Kiendler-Scharr, A., Kubelová, L., Lunder, C.,
- 420 Maasikmets, M., Makeš, O., Malaguti, A., Mihalopoulos, N., Nicolas, J. B., O'Dowd, C.,
- Ovadnevaite, J., Petralia, E., Poulain, L., Priestman, M., Riffault, V., Ripoll, A., Schlag, P.,
- 422 Schwarz, J., Sciare, J., Slowik, J., Sosedova, Y., Stavroulas, I., Teinemaa, E., Via, M., Vodička,
- 423 P., Williams, P. I., Wiedensohler, A., Young, D. E., Zhang, S., Favez, O., Minguillón, M. C., and
- 424 Prevot, A. S. H.: A European aerosol phenomenology 7: High-time resolution chemical

- characteristics of submicron particulate matter across Europe, Atmos Environ X, 10, 100108,
- 426 https://doi.org/10.1016/J.AEAOA.2021.100108, 2021.
- Canonaco, F., Tobler, A., Chen, G., Sosedova, Y., Slowik, J. G., Bozzetti, C., Daellenbach, K. R.,
- 428 El Haddad, I., Crippa, M., Huang, R.-J., Furger, M., Baltensperger, U., and Prévôt, A. S. H.: A
- 429 new method for long-term source apportionment with time-dependent factor profiles and
- 430 uncertainty assessment using SoFi Pro: application to 1 year of organic aerosol data, Atmos Meas
- 431 Tech, 14, 923–943, https://doi.org/10.5194/amt-14-923-2021, 2021.
- 432 deweather: Remove the influence of weather on air quality data: https://openair-
- project.github.io/deweather/, last access: 24 April 2025.
- Chebaicheb, H., de Brito, J. F., Amodeo, T., Couvidat, F., Petit, J.-E., Tison, E., Abbou, G., Baudic,
- 435 A., Chatain, M., Chazeau, B., Marchand, N., Falhun, R., Francony, F., Ratier, C., Grenier, D.,
- Vidaud, R., Zhang, S., Gille, G., Meunier, L., Marchand, C., Riffault, V., and Favez, O.: Multiyear
- high-temporal-resolution measurements of submicron aerosols at 13 French urban sites: data
- 438 processing and chemical composition, Earth Syst Sci Data, 16, 5089–5109,
- 439 https://doi.org/10.5194/essd-16-5089-2024, 2024.
- Chen, G., Canonaco, F., Tobler, A., Aas, W., Alastuey, A., Allan, J., Atabakhsh, S., Aurela, M.,
- Baltensperger, U., Bougiatioti, A., De Brito, J. F., Ceburnis, D., Chazeau, B., Chebaicheb, H.,
- Daellenbach, K. R., Ehn, M., El Haddad, I., Eleftheriadis, K., Favez, O., Flentje, H., Font, A.,
- 443 Fossum, K., Freney, E., Gini, M., Green, D. C., Heikkinen, L., Herrmann, H., Kalogridis, A.-C.,
- Keernik, H., Lhotka, R., Lin, C., Lunder, C., Maasikmets, M., Manousakas, M. I., Marchand, N.,
- Marin, C., Marmureanu, L., Mihalopoulos, N., Močnik, G., Nęcki, J., O'Dowd, C., Ovadnevaite,
- J., Peter, T., Petit, J.-E., Pikridas, M., Matthew Platt, S., Pokorná, P., Poulain, L., Priestman, M.,
- 447 Riffault, V., Rinaldi, M., Różański, K., Schwarz, J., Sciare, J., Simon, L., Skiba, A., Slowik, J. G.,

- Sosedova, Y., Stavroulas, I., Styszko, K., Teinemaa, E., Timonen, H., Tremper, A., Vasilescu, J.,
- Via, M., Vodička, P., Wiedensohler, A., Zografou, O., Cruz Minguillón, M., and Prévôt, A. S. H.:
- 450 European aerosol phenomenology 8: Harmonised source apportionment of organic aerosol using
- 451 22 Year-long ACSM/AMS datasets, Environ Int, 166, 107325,
- 452 https://doi.org/10.1016/j.envint.2022.107325, 2022.
- 453 Crippa, M., DeCarlo, P. F., Slowik, J. G., Mohr, C., Heringa, M. F., Chirico, R., Poulain, L., Freutel,
- 454 F., Sciare, J., Cozic, J., Di Marco, C. F., Elsasser, M., Nicolas, J. B., Marchand, N., Abidi, E.,
- Wiedensohler, A., Drewnick, F., Schneider, J., Borrmann, S., Nemitz, E., Zimmermann, R.,
- 456 Jaffrezo, J.-L., Prévôt, A. S. H., and Baltensperger, U.: Wintertime aerosol chemical composition
- and source apportionment of the organic fraction in the metropolitan area of Paris, Atmos Chem
- 458 Phys, 13, 961–981, https://doi.org/10.5194/acp-13-961-2013, 2013.
- Daellenbach, K. R., Uzu, G., Jiang, J., Cassagnes, L.-E., Leni, Z., Vlachou, A., Stefenelli, G.,
- 460 Canonaco, F., Weber, S., Segers, A., Kuenen, J. J. P., Schaap, M., Favez, O., Albinet, A.,
- 461 Aksoyoglu, S., Dommen, J., Baltensperger, U., Geiser, M., El Haddad, I., Jaffrezo, J.-L., and
- Prévôt, A. S. H.: Sources of particulate-matter air pollution and its oxidative potential in Europe,
- 463 Nature, 587, 414–419, https://doi.org/10.1038/s41586-020-2902-8, 2020.
- 464 Defra: Use of domestic fuels in the hospitality sector a qualitative review of hospitality
- businesses, 2023.
- Dominici, F., Peng, R. D., Bell, M. L., Pham, L., McDermott, A., Zeger, S. L., and Samet, J. M.:
- 467 Fine Particulate Air Pollution and Hospital Admission for Cardiovascular and Respiratory
- 468 Diseases, JAMA, 295, 1127, https://doi.org/10.1001/jama.295.10.1127, 2006.
- Europe's air quality status 2024:

- 470 Fröhlich, R., Cubison, M. J., Slowik, J. G., Bukowiecki, N., Prévôt, A. S. H., Baltensperger, U.,
- 471 Schneider, J., Kimmel, J. R., Gonin, M., Rohner, U., Worsnop, D. R., and Jayne, J. T.: The ToF-
- 472 ACSM: a portable aerosol chemical speciation monitor with TOFMS detection, Atmos Meas Tech,
- 473 6, 3225–3241, https://doi.org/10.5194/amt-6-3225-2013, 2013.
- 474 Gamelas, C. A., Canha, N., Vicente, A., Silva, A., Borges, S., Alves, C., Kertesz, Z., and Almeida,
- 475 S. M.: Source apportionment of PM2.5 before and after COVID-19 lockdown in an urban-
- 476 industrial area of the Lisbon metropolitan area, Portugal, Urban Clim, 49, 101446,
- 477 https://doi.org/10.1016/j.uclim.2023.101446, 2023.
- Hass-Mitchell, T., Joo, T., Rogers, M., Nault, B. A., Soong, C., Tran, M., Seo, M., Machesky, J.
- 479 E., Canagaratna, M., Roscioli, J., Claflin, M. S., Lerner, B. M., Blomdahl, D. C., Misztal, P. K.,
- Ng, N. L., Dillner, A. M., Bahreini, R., Russell, A., Krechmer, J. E., Lambe, A., and Gentner, D.
- 481 R.: Increasing Contributions of Temperature-Dependent Oxygenated Organic Aerosol to
- 482 Summertime Particulate Matter in New York City, ACS ES&T Air, 1, 113-128,
- 483 https://doi.org/10.1021/acsestair.3c00037, 2024.
- 484 Hong Kong EPD: Control of Oily Fume and Cooking Odour from Restaurants and Food Business,
- 485 2024.
- Hu, R., Wang, S., Zheng, H., Zhao, B., Liang, C., Chang, X., Jiang, Y., Yin, R., Jiang, J., and Hao,
- 487 J.: Variations and Sources of Organic Aerosol in Winter Beijing under Markedly Reduced
- 488 Anthropogenic Activities During COVID-2019, Environ Sci Technol, 56, 6956–6967,
- 489 https://doi.org/10.1021/acs.est.1c05125, 2022.
- 490 IPCC: Climate Change 2021 The Physical Science Basis, Cambridge University Press,
- 491 https://doi.org/10.1017/9781009157896, 2021.

- Jayne, J. T., Leard, D. C., Zhang, X., Davidovits, P., Smith, K. A., Kolb, C. E., and Worsnop, D.
- 493 R.: Development of an Aerosol Mass Spectrometer for Size and Composition Analysis of
- 494 Submicron Particles, Aerosol Science and Technology, 33, 49-70,
- 495 https://doi.org/10.1080/027868200410840, 2000.
- 496 Jeong, C.-H., Yousif, M., and Evans, G. J.: Impact of the COVID-19 lockdown on the chemical
- 497 composition and sources of urban PM2.5, Environmental Pollution, 292, 118417,
- 498 https://doi.org/10.1016/j.envpol.2021.118417, 2022.
- Jimenez, J. L., Canagaratna, M. R., Donahue, N. M., Prevot, A. S. H. H., Zhang, Q., Kroll, J. H.,
- DeCarlo, P. F., Allan, J. D., Coe, H., Ng, N. L., Aiken, A. C., Docherty, K. S., Ulbrich, I. M.,
- Grieshop, A. P., Robinson, A. L., Duplissy, J., Smith, J. D., Wilson, K. R., Lanz, V. A., Hueglin,
- 502 C., Sun, Y. L., Tian, J., Laaksonen, A., Raatikainen, T., Rautiainen, J., Vaattovaara, P., Ehn, M.,
- Kulmala, M., Tomlinson, J. M., Collins, D. R., Cubison, M. J., Dunlea, J., Huffman, J. A., Onasch,
- T. B., Alfarra, M. R., Williams, P. I., Bower, K., Kondo, Y., Schneider, J., Drewnick, F., Borrmann,
- 505 S., Weimer, S., Demerjian, K., Salcedo, D., Cottrell, L., Griffin, R., Takami, A., Miyoshi, T.,
- Hatakeyama, S., Shimono, A., Sun, J. Y., Zhang, Y. M., Dzepina, K., Kimmel, J. R., Sueper, D.,
- Jayne, J. T., Herndon, S. C., Trimborn, A. M., Williams, L. R., Wood, E. C., Middlebrook, A. M.,
- Kolb, C. E., Baltensperger, U., Worsnop, D. R., Dunlea, E. J., Huffman, J. A., Onasch, T. B.,
- Alfarra, M. R., Williams, P. I., Bower, K., Kondo, Y., Schneider, J., Drewnick, F., Borrmann, S.,
- Weimer, S., Demerjian, K., Salcedo, D., Cottrell, L., Griffin, R., Takami, A., Miyoshi, T.,
- Hatakeyama, S., Shimono, A., Sun, J. Y., Zhang, Y. M., Dzepina, K., Kimmel, J. R., Sueper, D.,
- Jayne, J. T., Herndon, S. C., Trimborn, A. M., Williams, L. R., Wood, E. C., Middlebrook, A. M.,
- Kolb, C. E., Baltensperger, U., and Worsnop, D. R.: Evolution of Organic Aerosols in the
- 514 Atmosphere, Science (1979), 326, 1525–1529, https://doi.org/10.1126/science.1180353, 2009.

- Joo, T., Rogers, M. J., Soong, C., Hass-Mitchell, T., Heo, S., Bell, M. L., Ng, N. L., and Gentner,
- D. R.: Aged and Obscured Wildfire Smoke Associated with Downwind Health Risks, Environ Sci
- 517 Technol Lett, 11, 1340–1347, https://doi.org/10.1021/acs.estlett.4c00785, 2024.
- Kelly, F. J. and Fussell, J. C.: Size, source and chemical composition as determinants of toxicity
- 519 attributable to ambient particulate matter, Atmos Environ, 60, 504–526,
- 520 https://doi.org/10.1016/j.atmosenv.2012.06.039, 2012.
- Laj, P., Lund Myhre, C., Riffault, V., Amiridis, V., Fuchs, H., Eleftheriadis, K., Petäjä, T., Salameh,
- 522 T., Kivekäs, N., Juurola, E., Saponaro, G., Philippin, S., Cornacchia, C., Alados Arboledas, L.,
- Baars, H., Claude, A., De Mazière, M., Dils, B., Dufresne, M., Evangeliou, N., Favez, O., Fiebig,
- M., Haeffelin, M., Herrmann, H., Höhler, K., Illmann, N., Kreuter, A., Ludewig, E., Marinou, E.,
- Möhler, O., Mona, L., Eder Murberg, L., Nicolae, D., Novelli, A., O'Connor, E., Ohneiser, K.,
- Petracca Altieri, R. M., Picquet-Varrault, B., van Pinxteren, D., Pospichal, B., Putaud, J.-P.,
- Reimann, S., Siomos, N., Stachlewska, I., Tillmann, R., Voudouri, K. A., Wandinger, U.,
- Wiedensohler, A., Apituley, A., Comerón, A., Gysel-Beer, M., Mihalopoulos, N., Nikolova, N.,
- 529 Pietruczuk, A., Sauvage, S., Sciare, J., Skov, H., Svendby, T., Swietlicki, E., Tonev, D., Vaughan,
- 530 G., Zdimal, V., Baltensperger, U., Doussin, J.-F., Kulmala, M., Pappalardo, G., Sorvari Sundet, S.,
- and Vana, M.: Aerosol, Clouds and Trace Gases Research Infrastructure (ACTRIS): The European
- Research Infrastructure Supporting Atmospheric Science, Bull Am Meteorol Soc, 105, E1098–
- 533 E1136, https://doi.org/10.1175/BAMS-D-23-0064.1, 2024.
- Liu, F., Joo, T., Ditto, J. C., Saavedra, M. G., Takeuchi, M., Boris, A. J., Yang, Y., Weber, R. J.,
- 535 Dillner, A. M., Gentner, D. R., and Ng, N. L.: Oxidized and Unsaturated: Key Organic Aerosol
- 536 Traits Associated with Cellular Reactive Oxygen Species Production in the Southeastern United
- 537 States, Environ Sci Technol, 57, 14150–14161, https://doi.org/10.1021/acs.est.3c03641, 2023.

- 538 Middlebrook, A. M., Bahreini, R., Jimenez, J. L., and Canagaratna, M. R.: Evaluation of
- 539 Composition-Dependent Collection Efficiencies for the Aerodyne Aerosol Mass Spectrometer
- 540 using Field Data, Aerosol Science and Technology, 46, 258–271,
- 541 https://doi.org/10.1080/02786826.2011.620041, 2012.
- Mohr, C., Huffman, J. A., Cubison, M. J., Aiken, A. C., Docherty, K. S., Kimmel, J. R., Ulbrich,
- I. M., Hannigan, M., and Jimenez, J. L.: Characterization of primary organic aerosol emissions
- 544 from meat cooking, trash burning, and motor vehicles with high-resolution aerosol mass
- spectrometry and comparison with ambient and chamber observations, Environ Sci Technol, 43,
- 546 2443–2449, https://doi.org/10.1021/ES8011518/SUPPL\_FILE/ES8011518\_SI\_001.PDF, 2009.
- Ng, N. L., Herndon, S. C., Trimborn, A., Canagaratna, M. R., Croteau, P. L., Onasch, T. B., Sueper,
- D., Worsnop, D. R., Zhang, Q., Sun, Y. L., and Jayne, J. T.: An Aerosol Chemical Speciation
- Monitor (ACSM) for Routine Monitoring of the Composition and Mass Concentrations of
- 550 Ambient Aerosol, Aerosol Science and Technology, 45, 780-794,
- 551 https://doi.org/10.1080/02786826.2011.560211, 2011.
- ONS: GDP and events in history: how the COVID-19 pandemic shocked the UK economy, 2022.
- Petit, J.-E., Dupont, J.-C., Favez, O., Gros, V., Zhang, Y., Sciare, J., Simon, L., Truong, F.,
- Bonnaire, N., Amodeo, T., Vautard, R., and Haeffelin, M.: Response of atmospheric composition
- to COVID-19 lockdown measures during spring in the Paris region (France), Atmos Chem Phys,
- 556 21, 17167–17183, https://doi.org/10.5194/acp-21-17167-2021, 2021.
- Pye, H. O. T., Ward-Caviness, C. K., Murphy, B. N., Appel, K. W., and Seltzer, K. M.: Secondary
- organic aerosol association with cardiorespiratory disease mortality in the United States, Nat
- 559 Commun, 12, 7215, https://doi.org/10.1038/s41467-021-27484-1, 2021.

- 560 Seinfeld, J. H., Wiley, J., and Pandis, S. N.: ATMOSPHERIC From Air Pollution to Climate
- 561 Change SECOND EDITION, 628–674 pp., 2006.
- Tian, J., Wang, Q., Zhang, Y., Yan, M., Liu, H., Zhang, N., Ran, W., and Cao, J.: Impacts of
- primary emissions and secondary aerosol formation on air pollution in an urban area of China
- 564 during the COVID-19 lockdown, Environ Int, 150, 106426,
- 565 https://doi.org/10.1016/j.envint.2021.106426, 2021.
- Tobler, A. K., Skiba, A., Wang, D. S., Croteau, P., Styszko, K., Necki, J., Baltensperger, U.,
- 567 Slowik, J. G., and Prévôt, A. S. H.: Improved chloride quantification in quadrupole aerosol
- 568 chemical speciation monitors (Q-ACSMs), Atmos Meas Tech, 13, 5293–5301,
- 569 https://doi.org/10.5194/amt-13-5293-2020, 2020.
- 570 Transport for London: Travel in London Report 13, 2020.
- Vasilakopoulou, C. N., Matrali, A., Skyllakou, K., Georgopoulou, M., Aktypis, A., Florou, K.,
- Kaltsonoudis, C., Siouti, E., Kostenidou, E., Błaziak, A., Nenes, A., Papagiannis, S., Eleftheriadis,
- K., Patoulias, D., Kioutsioukis, I., and Pandis, S. N.: Rapid transformation of wildfire emissions
- to harmful background aerosol, NPJ Clim Atmos Sci, 6, 218, https://doi.org/10.1038/s41612-023-
- 575 00544-7, 2023.
- Via, M., Chen, G., Canonaco, F., Daellenbach, K. R., Chazeau, B., Chebaicheb, H., Jiang, J.,
- Keernik, H., Lin, C., Marchand, N., Marin, C., O'dowd, C., Ovadnevaite, J., Petit, J.-E., Pikridas,
- 578 M., Riffault, V., Sciare, J., Slowik, J. G., Simon, L., Vasilescu, J., Zhang, Y., Favez, O., Prévôt,
- A. S. H., Alastuey, A., and Cruz Minguillón, M.: Rolling vs. seasonal PMF: Real-world multi-site
- and synthetic dataset comparison, Atmos Meas Tech, 15, https://doi.org/10.5194/amt-15-5479-
- 581 2022, 2022.

- Wei, Y., Qiu, X., Yazdi, M. D., Shtein, A., Shi, L., Yang, J., Peralta, A. A., Coull, B. A., and
- 583 Schwartz, J. D.: The Impact of Exposure Measurement Error on the Estimated Concentration-
- Response Relationship between Long-Term Exposure to PM2.5 and Mortality, Environ Health
- 585 Perspect, 130, https://doi.org/10.1289/EHP10389, 2022.
- Wei, Y., Feng, Y., Danesh Yazdi, M., Yin, K., Castro, E., Shtein, A., Qiu, X., Peralta, A. A., Coull,
- 587 B. A., Dominici, F., and Schwartz, J. D.: Exposure-response associations between chronic
- 588 exposure to fine particulate matter and risks of hospital admission for major cardiovascular
- diseases: population based cohort study, BMJ, e076939, https://doi.org/10.1136/bmj-2023-076939,
- 590 2024.
- World Health Organization: WHO global air quality guidelines. Particulate matter (PM2.5 and
- 592 PM10), ozone, nitrogen dioxide, sulfur dioxide and carbon monoxide., Geneva, 2021.
- 593 Xu, J., Ge, X., Zhang, X., Zhao, W., Zhang, R., and Zhang, Y.: COVID-19 Impact on the
- 594 Concentration and Composition of Submicron Particulate Matter in a Typical City of Northwest
- 595 China, Geophys Res Lett, 47, https://doi.org/10.1029/2020GL089035, 2020.
- Zhang, Qi., Jimenez, J. L., Canagaratna, M. R., Allan, J. D., Coe, H., Ulbrich, I., Alfarra, M. R.,
- Takami, A., Middlebrook, A. M., Sun, Y. L., Dzepina, K., Dunlea, E., Docherty, K., DeCarlo, P.
- 598 F., Salcedo, D., Onasch, T., Jayne, J. T., Miyoshi, T., Shimono, A., Hatakeyama, S., Takegawa,
- N., Kondo, Y., Schneider, J., Drewnick, F., Borrmann, S., Weimer, S., Demerjian, K., Williams,
- P., Bower, K., Bahreini, R., Cottrell, L., Griffin, R. J., Rautiainen, J., Sun, J. Y., Zhang, Y. M., and
- Worsnop, D. R.: Ubiquity and dominance of oxygenated species in organic aerosols in
- anthropogenically-influenced Northern Hemisphere midlatitudes, Geophys Res Lett, 34, n/a-n/a,
- 603 https://doi.org/10.1029/2007GL029979, 2007.